Soft Matter

www.rsc.org/softmatter

Volume 9 | Number 29 | 7 August 2013 | Pages 6543–7202

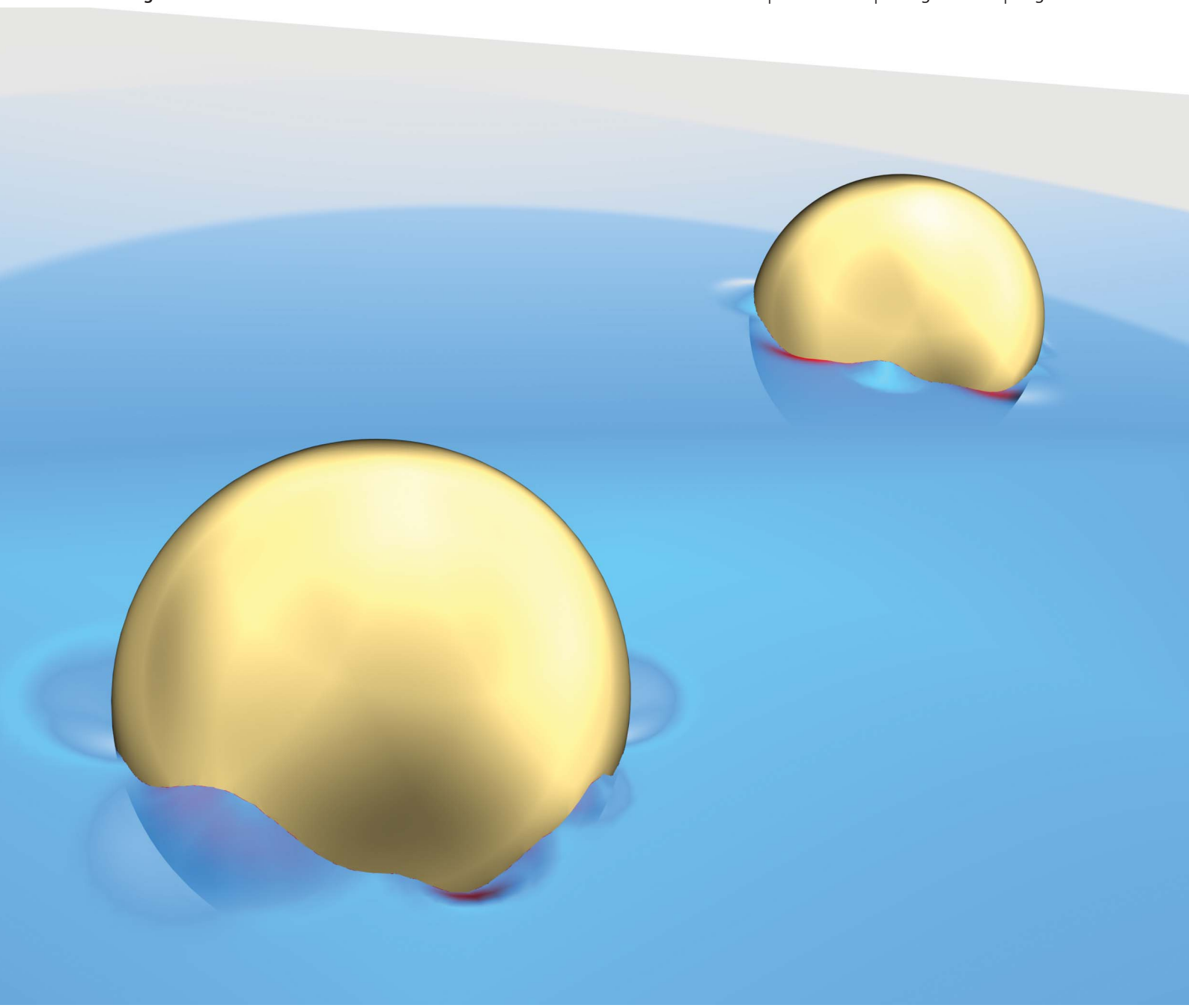

ISSN 1744-683X

RSC Publishing

REVIEW ARTICLE

Daeyeon Lee *et al.*

Amphiphilic Janus particles at fluid interfaces

Soft Matter

RSC Publishing

REVIEW

View Article Online
View Journal | View Issue

Amphiphilic Janus particles at fluid interfaces

Cite this: *Soft Matter*, 2013, **9**, 6604

Ankit Kumar, Bum Jun Park,† Fuquan Tu and Daeyeon Lee*

Janus particles are colloids that have both hydrophilic and hydrophobic faces. Recent advances in particle synthesis enable the generation of geometrically and chemically anisotropic Janus particles with high uniformity and precision. These amphiphilic particles are similar to molecular surfactants in many aspects; they self-assemble in bulk media and also readily attach to fluid interfaces. These particles, just like molecular surfactants, could potentially function as effective stabilizers for various multiphasic systems such as emulsions and foams. In particular, just as the shape and chemical composition have a significant impact on the surfactancy of molecular amphiphiles, the ability to control the shape and wetting properties of Janus particles could provide a unique opportunity to control their surface activity. In this review, we first examine the recent developments in using amphiphilic Janus particles as colloid surfactants to stabilize multiphasic mixtures such as emulsions. These results have motivated a number of detailed investigations aimed at understanding the behaviour of Janus particles at fluid–fluid interfaces at the microscopic level, which we highlight. This review also discusses the importance of controlling the shape of Janus particles, which has a drastic impact on their behaviour at fluid interfaces. We conclude this review by presenting outlook on the future directions and outstanding problems that warrant further study to fully enable the utilization of Janus particles as colloid surfactants in practical applications.

Received 22nd January 2013
Accepted 25th March 2013

DOI: 10.1039/c3sm50239b

www.rsc.org/softmatter

Introduction

In 1991, in his Nobel lecture titled "Soft Matter", Pierre-Gilles de Gennes described a new 'animal' called the 'Janus grain'. These are particles with opposite polarities on the two hemispheres.[1] According to de Gennes, these Janus colloids, although similar to surfactants in their amphiphilicity, should exhibit a unique property that is not observed in molecular amphiphiles when they are placed at an air–water interface. While a film of surfactant molecules at the interface would be dense, Janus particles would form a film with large interstices, through which chemical exchange can occur between the two phases. This 'breathable skin' property, along with many others, makes Janus particles unique and potentially useful in practical applications. Likely due to the lack of effective methods for synthesizing these anisotropic particles, however, this prescience idea did not gain immediate attention from the scientific community, as evidenced by a limited number of publications in this area in the early 1990s.[2–6] With the recent

Department of Chemical and Biomolecular Engineering, University of Pennsylvania, Philadelphia, PA 19104, USA. E-mail: daeyeon@seas.upenn.edu; Tel: +1-215-573-4521

† Current address: Department of Chemical Engineering, Kyung Hee University, Yongin-si, Gyeonggi-do, 446-701, South Korea.

Ankit Kumar obtained his Bachelors' degree in Chemical Engineering from Indian Institute of Technology, Bombay in 2011. He is currently pursuing a doctoral degree in the Chemical and Biomolecular Engineering Department at the University of Pennsylvania. His research focuses on the behaviour of amphiphilic particles at fluid–fluid interfaces.

Bum Jun Park obtained his Ph.D. in 2010 at the University of Delaware. After spending two years as a postdoctoral researcher at the University of Pennsylvania, he is currently an assistant professor in the Department of Chemical Engineering at Kyung Hee University. His research interests focus on interactions, microstructures and rheology of colloidal particles at fluid–fluid interfaces.

development of a plethora of synthesis techniques[3,7–16] and motivation from a wide array of potential applications, the field of Janus particles is now at the forefront of soft matter research.

The anisotropy in wetting, magnetic, catalytic, optical and electrical properties of Janus particles leads to unique behaviour and properties that are not observed in homogeneous particles of similar dimensions. In particular, their ability to self-assemble in a bulk medium such as water is analogous to the self-assembly of molecular amphiphiles and has been explored in considerable detail in recent years.[10,15,17–22] Self-propulsion utilizing chemical reactions on one side of these anisotropic colloids is another recent development that may have implications in targeted drug delivery.[23–29] These recent observations and results have inspired new areas of potential applications for these Janus particles, which provide improved performance over conventional homogeneous colloidal particles, in diverse fields such as biomedicine,[30–34] electronics and sensors,[35–40] optics,[41–45] super-hydrophobic textiles,[46,47] and many others.

One of the most intriguing applications of Janus particles is their use as solid surfactants for the stabilization of multiphasic mixtures such as emulsions and foams.[1,10,48] In fact, de Gennes' vision to form a breathable skin made of a Janus particle monolayer at a fluid–fluid interface to allow for the exchange of matter between the two fluid phases has recently been realized in a study by Faria and co-workers.[49] Here, the amphiphilicity of Janus particles was further exploited to enhance the phase-selectivity of a biofuel refining process. They explored metal-supporting Janus particles as interfacial catalysts. Two types of Janus particles – one with catalyst on both faces, and the other with catalyst only on the hydrophobic side – were used to stabilize oil-in-water emulsions with the oil phase containing benzaldehyde and the water phase containing glutaraldehyde, as shown in Fig. 1.[49] It was shown that Janus particles with catalyst just on the hydrophobic face had better phase selectivity than the particles with catalyst on both sides. Such phase-selectivity is especially important for bio-fuel refining processes involving numerous reactions where phase-selectivity is crucial to achieve high yield and to avoid competing reactions from hampering product formation. They also described the advantages of using Janus particles as "interfacial catalyst emulsifiers" in achieving a high biofuel conversion because of high interfacial area and easy separation of the catalyst and reaction product.

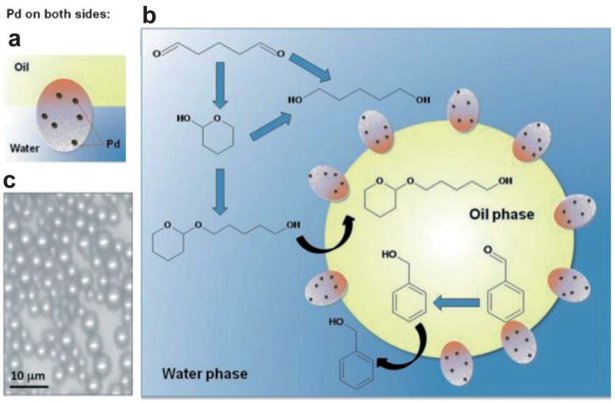

Fig. 1 (a) Schematic illustration of a Janus particle loaded with Pd catalyst on both sides. (b) Schematic representation of the hydrogenation reactions taking place in the oil and water phases, with particles sitting at the oil–water interface with catalyst on both sides of the Janus particles; (c) microscope image of the oil-in-water emulsions; Reprinted with permission from ref. 49.

Starting from de Gennes' vision of Janus particles forming a 'breathable skin' at a fluid interface to the latest applications of Janus particles as interfacial catalyst emulsifiers facilitating biofuel conversion, the field has witnessed tremendous scientific advances and activities in the last decade. Also significant

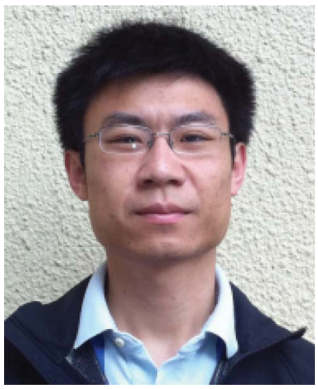

Fuquan Tu received his Bachelor's degree in Materials Science and Engineering at Tsinghua University (China) in 2010. He is now pursuing his Ph.D. in the Department of Chemical and Biomolecular Engineering at the University of Pennsylvania. His research focuses on using Janus particles as colloid surfactants and microfluidic generation of functional particles.

Daeyeon Lee received his B.S. in Chemical Engineering from Seoul National University in 2001 and received his Ph.D. in Chemical Engineering at MIT in 2007. After his Ph.D., Daeyeon was a postdoctoral fellow in the School of Engineering and Applied Sciences at Harvard University. Daeyeon joined the Department of Chemical and Biomolecular Engineering at the University of Pennsylvania in 2009 as an assistant professor. Daeyeon has won numerous awards including the 2010 Victor K. LaMer Award from ACS Colloid and Surface Chemistry Division, the NSF CAREER Award (2011), the 2011 Korean-American Scientists and Engineers Association Young Investigator Award, the 2012 KIChE President Young Investigator Award and the 2013 3M Nontenured Faculty Award.

advances in addressing important synthetic challenges, such as scalability and control over geometry, have been made, which serve as a catalyst for further development in this area. To enable the engineering of amphiphilic Janus particles as solid surfactants for a variety of applications, a comprehensive understanding of the behaviour of Janus particles at fluid interfaces is imperative. Such a need motivates us to focus this review article on the current status of understanding of the interfacial behaviour of Janus particles. To learn more about the recent developments in the synthesis of Janus particles and other aspects such as their assembly in bulk media and their self-locomotion, we refer the readers to recent reviews that cover the relevant topics.[8–12,19,50,51] Readers interested in the interfacial behaviour of homogeneous particles are referred to ref. 52 and 53, which provide comprehensive reviews on this topic.

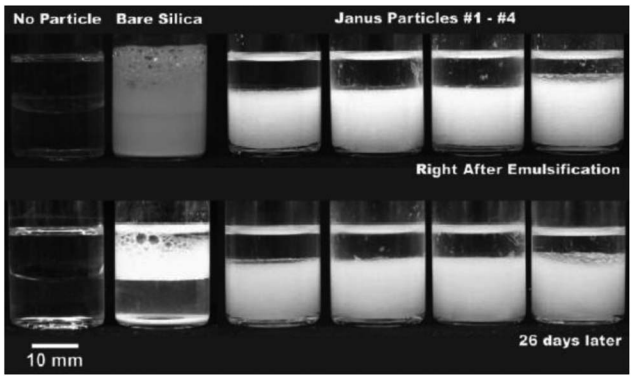

Fig. 3 Comparison between emulsion stabilization (left) without particles, (second column) with unmodified silica particles, and (third to last columns) with Janus particles. Images were taken immediately after and 26 days after emulsification. Reprinted with permission from ref. 10.

Janus particles as colloid surfactants

Studies focusing on the application of Janus particles as colloid surfactants have shown that these particles are able to stabilize emulsions and maintain their stability for an extended period of time, more effectively than homogeneous particles. For example, it was shown that Janus particles have significantly higher interfacial activity than their homogeneous counterparts, and thus, can effectively lower the interfacial tension between oil and water, as shown in Fig. 2.[54] Janus particles synthesized by selective surface modification of hydrophilic silica particles were shown to effectively stabilize oil droplets in water.[55] In addition, oil-in-water emulsions stabilized with Janus particles showed superior long-term stability compared to those stabilized with homogeneous silica particles, as shown in Fig. 3.[10]

Non-spherical Janus particles also have been explored as emulsifiers. Janus dumbbells (or dimers) made of two partially fused spheres of opposing wettability (Fig. 4) have been shown to exhibit considerable "surfactancy".[56] It was proposed that the shape (*i.e.*, the ratio of the size of the two spheres) could play an important role in determining the surface activity of these Janus dumbbells. These particles have the tendency to cover the interface with closely packed arrangements. Another remarkable observation was the stabilization of emulsion droplets that are non-spherical, as shown in Fig. 4 (right), which was hypothesized to occur due to jamming of dumbbells at the interface in time scales smaller than the relaxation time of the droplets. In another study, amphiphilic Janus nanosheets were explored for emulsion stabilization.[57] These plate-like Janus particles were found to be effective in decreasing the surface tension, demonstrated by a decrease in the size of emulsion droplets formed using these particles as emulsifiers. When used in emulsion polymerization, increasing the concentration of these amphiphilic nanosheets led to a decrease in the size of the synthesized polystyrene particles.

Janus particles have also been used to facilitate the formation of new materials. It was demonstrated that Janus particles could compatibilize polymer blends much more effectively than block and graft copolymers, which, currently, are the state-of-the-art compatibilizers.[58] The effectiveness of Janus particles as polymer compatibilizers was attributed to their tendency to readily adsorb to polymer–polymer interfaces and to remain at the interfaces without micellization, even under high temperature and high shear conditions. Another study showed that

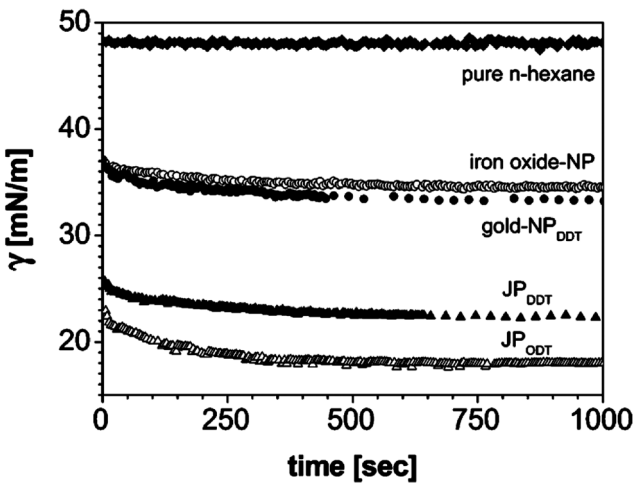

Fig. 2 Comparison between homogeneous iron-oxide nanoparticles and 1-dodecanethiol (DDT) modified Janus nanoparticles in decreasing the interfacial tension at a water–*n*-hexane interface. Reprinted with permission from ref. 54.

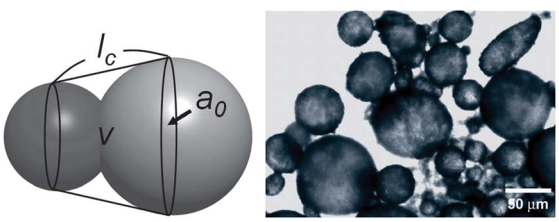

Fig. 4 (Left) Schematic illustration of a Janus dumbbell with a parameter used to define the packing parameter ($\left(P_{\text{packing}} = \frac{v}{a_0 l_c}\right)$) of a dumbbell; (right) non-spherical emulsion droplets formed by using amphiphilic dumbbells as colloid surfactants. Reprinted with permission from ref. 56.

when Janus particles were used as emulsifiers in mini-emulsion polymerization, no additives were required, unlike in Pickering emulsion polymerization using homogeneous particles.[59] Also, the size of the particles produced with Janus particles was shown to be very well controlled and monodisperse. The reason for such excellent performance of Janus particles as a stabilizer in emulsion polymerization was attributed to their strong tendency to adsorb to the oil–water interfaces.

In addition to these advances in experiments, a simulation study using dissipative particle dynamics was used to study the mechanism of coalescence between two emulsion droplets stabilized with Janus particles.[60] The nanoparticle surface coverage, their surface activity and the stability of the film forming between two coalescing droplets were found to be extremely critical in determining the stability of emulsions. At a comparable coverage, Janus nanoparticle-covered emulsions showed superior emulsion stability over those stabilized with homogeneous nanoparticles because of the high surface activity of Janus particles.

The main reason that Janus particles are able to stabilize emulsions more effectively than homogenous particles can be explained by their strong attachment to fluid interfaces. Due to the amphiphilicity of Janus particles, the desorption energy of a Janus particle from a fluid interface can be as large as three times that of a homogeneous particle.[61] Further extending this work, it was theoretically shown that spherical Janus particles can lead to the formation of thermodynamically stable Pickering emulsions.[62] In contrast, Pickering emulsions stabilized with homogeneous particles generally are only kinetically stable. The large attachment energy of Janus particles to fluid interfaces is able to overcome the energy penalty that is associated with creating a bare oil–water surface area during emulsion formation.

Behaviour of individual Janus spheres at fluid–fluid interfaces

As summarized above, a number of studies have demonstrated the promise of using Janus particles as colloid surfactants in the stabilization of multiphasic mixtures such as emulsions. Inevitably, Janus particles come in contact with fluid–fluid interfaces in these applications. At a fluid interface, there is an imbalance of cohesive interactions, which leads to the development of a tension that minimizes the interfacial area between two fluid phases. This tendency to reduce the surface area can be quantified as surface energy per unit area and is known as the surface (interfacial) tension.[63] The existence of this energy has a profound effect on the behaviour of particles at the interface and the properties of the interface as a whole. It has been proposed that for Janus particles to be effective in stabilizing emulsions, it is very important for them to be oriented in the 'right' way; that is, they should have their hydrophilic part facing the water phase and hydrophobic part facing the oil phase.[64] An in-depth analysis of the interfacial behaviour of Janus particles at the single particle level, thus, is an important step in providing insights into their efficacy as colloid surfactants in emulsion/foam stabilization.

One of the first discussions on the behaviour, and specifically on the positioning of individual Janus particles at interfaces, was reported by Casagrande *et al.*[3] In this paper they showed that while homogenous beads exhibit varying contact angles at the interface depending on their surface properties, symmetric Janus spheres, with equal hydrophobic and hydrophilic areas, exhibit a constant contact angle of 90°. The observation was rationalized by semi-quantitative energetic arguments that the equilibrium position of colloidal particles at fluid interfaces is dependent on the minimization of two energy components – E_{SL} (interfacial energy between the solid and liquid) and E_{LL} (interfacial energy between the two liquid phases). While for homogeneous particles, these effects act against each other, that is, when E_{SL} is minimized, E_{LL} is maximized and *vice versa*; for Janus particles, these effects are cooperative; that is, they work together to decrease the energy of the system leading to equatorial anchoring being the equilibrium configuration of symmetric Janus particles.

Ondarçuhu *et al.* performed an experimental and theoretical study on the positioning of Janus particles at fluid interfaces.[4] They showed through calculations that energetically, the most favourable position of a Janus particle is such that the interface is pinned at the Janus boundary, which is the wettability separation line (WSL) between the two regions, even for a chemically anisotropic Janus particle under appropriate circumstances. As shown in Fig. 5(b), although the WSL does not coincide with the equator of the particle, as long as it lies within a specific range, the energy minimum occurs when the interface becomes pinned at the WSL. This regime was identified as the Janus regime, which includes the symmetric and moderately asymmetric Janus particles. In contrast, when Janus particles are highly asymmetric they can be in the so-called homogeneous regime. These highly asymmetric Janus particles behave like homogeneous particles, despite the fact that they are chemically anisotropic because the ratio of areas of the two regions is either very large or very small. In these cases, the position for energy minimum corresponds to the same contact angle as the corresponding homogeneous particle as shown in Fig. 5(a) and (c), thereby exhibiting the behaviour of the homogeneous regime. Experiments using Janus particles with varying area ratios of hydrophilic and hydrophobic regions were performed and a transition in the regime was observed.

It was later shown, through energetic calculations, that a Janus particle, half hydrophobic and half hydrophilic, can be up to three times more surface active than a corresponding homogeneous particle.[61] Calculation of the energy to detach a single particle from an oil–water interface (*i.e.* detachment energy) was used to arrive at this important conclusion. The geometry shown in Fig. 6 was assumed for a generalized Janus particle, where the ratio of the hydrophobic and hydrophilic regions may not be 1 : 1.

Under the assumption of a flat interface, total surface free energy (E) for a Janus particle at the interface as a function of the angle β can be expressed as

$$E_A(\beta) = 2\pi R^2 \left[\gamma(\mathrm{AO})(1+\cos\alpha) + \gamma(\mathrm{PO})(\cos\beta - \cos\alpha) + \gamma(\mathrm{PW})(1-\cos\beta) - \frac{1}{2}\gamma(\mathrm{OW})\left(\sin^2\beta\right) \right] \text{ for } \beta \le \alpha \quad (1)$$

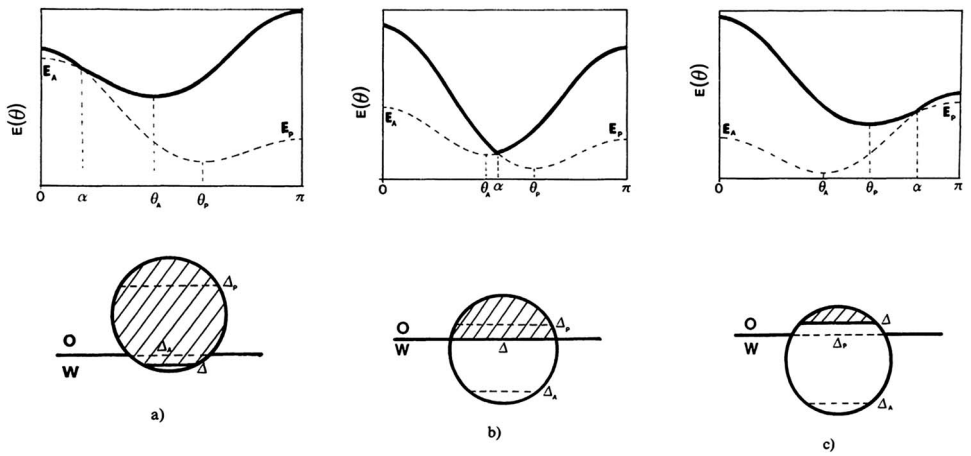

Fig. 5 The dotted lines represent E_A and E_P given by eqn (1) and (2), respectively. The solid lines represent the total surface free energy (E) for a Janus particle at the interface as a function of the angle β. Case (a) $\alpha < \theta_A < \theta_P$, case (b) $\theta_A < \alpha < \theta_P$, case (c) $\theta_A < \theta_P < \alpha$. Reprinted with permission from ref. 4.

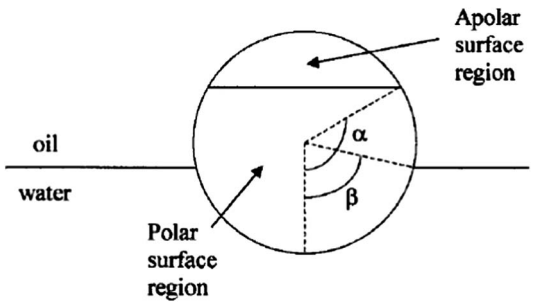

Fig. 6 Geometry of a Janus particle at an oil–water interface with parameters α and β that represent positions of the Janus boundary (WSL) and the interface, respectively. Reprinted with permission from ref. 61.

$$E_P(\beta) = 2\pi R^2\left[\gamma(\mathrm{AO})(1+\cos\beta) + \gamma(\mathrm{AW})(\cos\alpha - \cos\beta) + \gamma(\mathrm{PW})(1-\cos\alpha) - \frac{1}{2}\gamma(\mathrm{OW})\left(\sin^2\beta\right)\right] \text{ for } \beta \geq \alpha \quad (2)$$

where R is the particle radius and γ(ij) is the interfacial tension between phases i and j. Line tension effects on the three phase contact line were neglected in these calculations. The area weighted average contact angle is then defined as,

$$\theta_{\mathrm{avg}} = \frac{\theta_A(1+\cos\alpha) + \theta_P(1-\cos\alpha)}{2} \quad (3)$$

The particle amphiphilicity is changed from homogeneous to most amphiphilic surfaces and can be characterized by,

$$\Delta\theta = \frac{\theta_P - \theta_A}{2} \quad (4)$$

$\Delta\theta = 0^\circ$ corresponds to a homogeneous particle, whereas $\Delta\theta = 90^\circ$ corresponds to maximum possible amphiphilicity. It can be seen in Fig. 7 that the desorption energy of a Janus particle from the fluid interface increases with $\Delta\theta$ and that for the parameters considered for these theoretical calculations, a roughly three-fold increase in the desorption energy

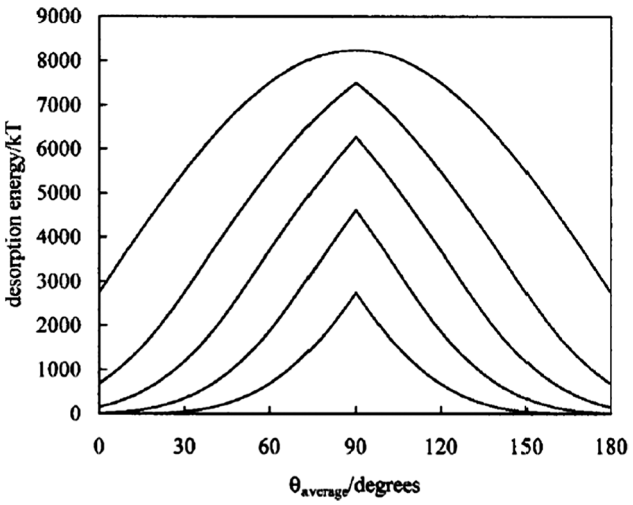

Fig. 7 Variation of desorption energy with area weighted contact angle for particles ($\alpha = 90^\circ$ and γ(OW) = 0.036 N m^{-1}). In order of increasing desorption energy, the curves correspond to $\Delta\theta$ = 0, 20, 40, 60 and 90°. Reprinted with permission from ref. 61.

can be achieved over that of a homogeneous particle of the same size.

To quantify the capability and efficiency of Janus particles as solid surfactants, the concept of Janus balance was introduced, by drawing analogy to the hydrophilic–lipophilic balance (HLB) of molecular surfactants.[65] It was defined as the dimensionless ratio of work to transfer an amphiphilic Janus particle from the oil–water interface to the oil phase, normalized by the work needed to move it to the water phase. According to this definition, the expression of Janus balance (J) can be obtained, ignoring the line tension and gravity effects, as follows:

$$J = \frac{\sin^2\alpha + 2\cos\theta_P(\cos\alpha - 1)}{\sin^2\alpha + 2\cos\theta_A(\cos\alpha + 1)} \quad (5)$$

J, therefore, depends on the nature and relative areas of the two regions of opposite wettabilities. If adsorption energy is defined

as the minimum of E_{oil} and E_{water}, then it can be seen from Fig. 8 that the highest adsorption energy is obtained for $J = 1$. Although no quantitative predictions were provided, it was suggested that the concept of Janus balance could be used in predicting self-assembly behaviour and design of Janus particles as effective emulsifiers.

The interaction of a single Janus nanoparticle with a fluid interface has also recently been studied using Monte Carlo simulation.[66] The results point out that the interaction between the nanoparticles and the interface is long-ranged due to the effective increase in the thickness of the interface due to the formation of capillary waves. Also in contrast to homogeneous nanoparticles, Janus nanoparticles showed an increase in stability at the interface, which was quantified in terms of detachment energy of the particle from the interface to one of the two bulk phases, when the affinity of each hemisphere with its corresponding favourable phase is increased. When the asymmetry in the wetting properties of Janus particles was increased, however, the stability decreased.

While the properties of Janus particles play a significant role in determining their behaviour at fluid–fluid interfaces, the importance of the interfacial curvature should not be ignored. Hirose *et al.* investigated the adsorption of Janus particles to a curved fluid–fluid interface.[67] They showed that the equilibrium contact angle of a Janus particle at a curved interface is determined by the geometry of the particle, its wettability, and also the interfacial curvature. In particular, a Janus particle, whose Janus boundary would have been pinned to a planar interface, can have the Janus boundary de-pinned from the interface if the radius of curvature of the interface is comparable to the size of the Janus particle. This de-pinning is caused by a high internal pressure (due to curvature-induced Laplace pressure) imposed on the particle when it is at the interface. They also found that there exists a preferred interfacial curvature for Janus particles due to volume energy exerted by the Laplace pressure when the particle satisfies certain conditions. The preferred interfacial curvature only occurs when the Janus boundary is pinned at the interface, and the window in which the preferred interfacial curvature can be observed is rather narrow.

It is important to note that while theoretical and experimental observations show that Janus particles dominantly adopt their equilibrium position at fluid interfaces, Janus particles at interfaces can be rotationally trapped in the 'wrong' orientation due to the presence of surface roughness.[64] Possible reasons for energy barrier to rotation may range from contact angle hysteresis to deformation of interface due to an irregular Janus boundary.

The interaction of individual Janus particles with fluid interfaces is fundamental in understanding how the microscopic behaviour of individual particles translates into the observable macroscopic properties. Another interaction, which likely plays a crucial role in shaping their overall macroscopic nature, is the lateral interactions between Janus particles when they are spread at the interface. The next section covers this important aspect of Janus particle behaviour at fluid interfaces.

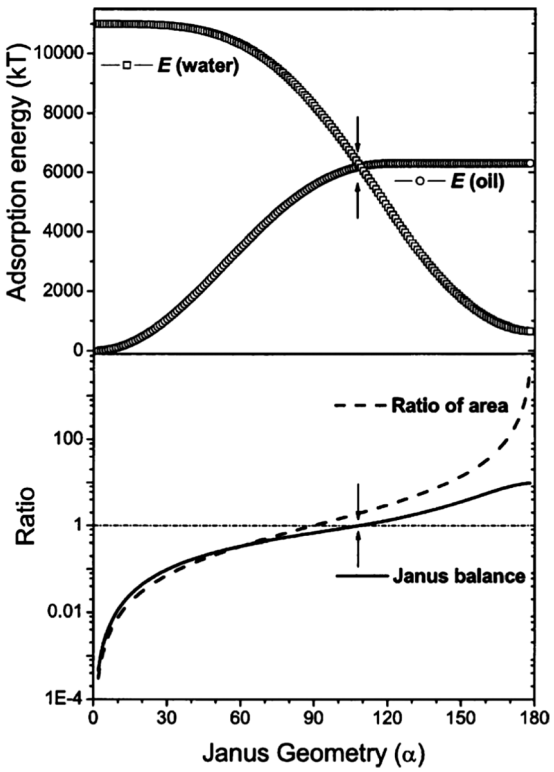

Fig. 8 Adsorption energy and Janus balance ratio for a Janus particle (10 nm, $\theta_A = 0°$, $\theta_P = 121°$, $T = 298$ K) showing $J = 1$ as the point of the highest adsorption energy. The dashed line is the ratio of the hydrophilic and hydrophobic areas of the Janus particle. Reprinted with permission from ref. 65.

Lateral interactions between Janus spheres at fluid interfaces

The presence and organization of solid particles at the interface between two immiscible fluids affect the static and dynamic properties of the interface.[67–69] The amphiphilicity of Janus particles could influence their arrangements at fluid interfaces, which would have a significant impact on their properties as colloid surfactants; therefore, a clear understanding of lateral interactions between Janus particles at fluid interfaces is crucial.

Janus particles and their interactions at fluid interfaces were studied in detail by Park *et al.*[70] They also explored the assembly behaviour of Janus particles and highlighted the striking difference between Janus and homogeneous particles. As can be seen in Fig. 9, while homogeneous particles show long-range repulsions, characterized by the formation of a hexagonal array of particles with a large interparticle spacing, Janus particles form a 'fractal-like' aggregate structure, suggesting that their interactions are pre-dominantly attractive.

Through particle-trajectory analysis, the interaction between pairs of Janus particles was experimentally measured to be on the order of $\sim 10^6\ k_B T$ and vary with the inter-particle separation distance (r) roughly as $U \sim r^{-4}$. Based on these observations, it was hypothesized that capillary interactions are responsible for the observed attraction and result from undulations in the three-phase contact line on the particle surface.

This hypothesis was inspired by previous work involving homogeneous particles at fluid–fluid interfaces.[71] Although

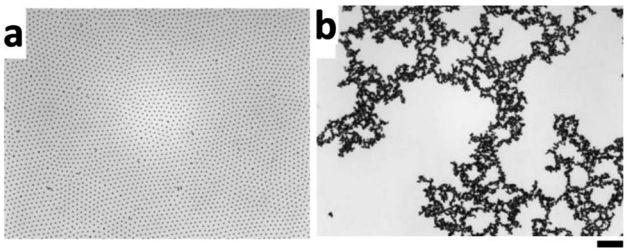

Fig. 9 Interface assembly of (a) homogeneous polystyrene (PS) particles and (b) PS particles with one hemisphere coated with Au and modified with 1-dodecanethiol (DDT) to make it hydrophobic. The scale bar is 100 μm. Reprinted in part from ref. 70.

small particles with perfectly uniform surface wettability are not expected to induce interface deformation, chemical heterogeneity or surface roughness of particles can lead to undulating three phase contact lines around particles trapped at the fluid interface.[72–74] Strong capillary attraction between these particles arises because the deformed interface represents extra surface area or energy, which the system minimizes by inducing aggregation among the particles. It was shown that for a 1 μm sphere with interface deformation of around 50 nm, the interaction energy between a pair of particles can be as high as $10^4\ k_BT$.

The interfacial profile around such a particle can be obtained by solving the Young–Laplace equation and can be expressed as:[72]

$$\Delta h(r,\varphi) = \left\{\frac{1}{r} \times \frac{\partial}{\partial r} r \frac{\partial}{\partial r} + \frac{1}{r^2}\frac{\partial^2}{\partial \varphi^2}\right\} h(r,\varphi) = 0 \qquad (6)$$

where $h(r,\varphi)$ is the height of interfacial undulation and (r,φ) are in the cylindrical coordinates. The corresponding solution can be written in the form of a multi-pole series expansion

$$h(r_c,\varphi) = \sum_{m=2}^{\infty} H_m \cos\left(m\left(\varphi - \varphi_{m,0}\right)\right) \qquad (7)$$

where m is defined as the order of the multipoles. The summation starts at $m = 2$ because $m = 0$ corresponds to the monopole which is negligible for systems with small Bond numbers (*i.e.*, gravitation force $\ll$ surface tension force). The dipole term ($m = 1$) is also negligible since the system has to satisfy the mechanical equilibrium condition. The first term in this expansion is, therefore, $m = 2$, which corresponds to a quadrupolar undulation. For the quadrupole-dominant interfacial undulation, the interaction energy between two particles as a function of inter-particle separations was shown to follow $U \sim r^{-4}$.[75] The dependence of experimentally obtained inter-particle potential between Janus particles, therefore, is consistent with the potential between two interface-trapped spheres that have random undulating three phase contact lines.[70,72]

When Janus particles, with sufficiently different wettabilities on the two faces, are at the interface of two fluids, a majority of them orient with their apolar face immersed in the oil phase and the polar face immersed in the water phase.[70] In such an orientation, it is energetically favourable for the fluid interface to be pinned at the Janus boundary. The line-of-sight evaporation approach that was used to generate Janus particles leads to a diffuse Janus boundary instead of an ideally smooth WSL.[41,75–77] Thus, the heterogeneity of the Janus boundary leads to undulations in the interface around the Janus particles and, in turn, capillary interactions between these particles, as schematically illustrated in Fig. 10.

Similar capillary interactions were also observed in another study involving Janus bubbles, which are essentially gas-filled solid particles that are roughly 50 μm in diameter, at an air–water interface.[75] Because of their buoyancy, these Janus bubbles offer a unique opportunity to study the behaviour of Janus particles at an air–water interface as originally envisioned by de Gennes.[1] More importantly, because of their size, it is straightforward to directly observe their interfacial behaviour *via* optical microscopy. In addition to the long-range attractive interactions leading to similar 'fractal-like' clusters, rotation and re-arrangement of Janus bubble clusters were observed during their assembly. This observation points towards directional anisotropy in the interactions between Janus bubbles.

This study also found that the magnitude of interactions between Janus bubbles increases with bubble size, which would be expected for particles interacting *via* capillary interactions as shown in Fig. 11.[75] While it was shown that the magnitude of interactions tends to increase with the particle size, the interactions between different pairs of equally sized Janus bubbles did not give the same magnitude of interactions. This observation was again attributed to the random nature of the undulating contact line on the Janus bubble surface, which would be different for each bubble.

The presence of undulating interfacial deformation around Janus bubbles was further confirmed by directly observing the interface profile using optical profilometry. Results provided evidence of concave and convex local undulations, indicated by white and red arrows in Fig. 12.[75] Also, capillary bridges can be seen in the regions between Janus bubbles as is expected for particles interacting through capillary interactions. In contrast to Janus bubbles, homogeneous bubbles show no significant unevenness in the menisci.

In summary, the long-range capillary attraction between Janus particles originates because of the random undulations in the three-phase contact lines around the Janus boundary. These undulations likely play a crucial role in determining the interactions between multiple particles and, in turn, the assembly and rheological properties of monolayers of Janus particles at fluid–fluid interfaces. Subsequently these macroscopic

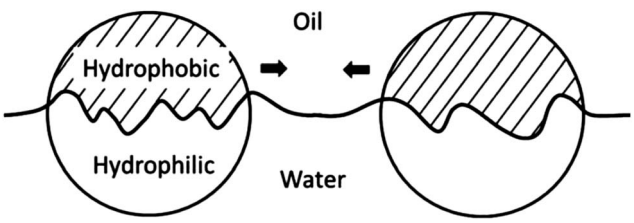

Fig. 10 Schematic illustration showing attractive interaction between Janus particles arising because of undulating contact lines (exaggerated for illustration). Reprinted in part from ref. 70.

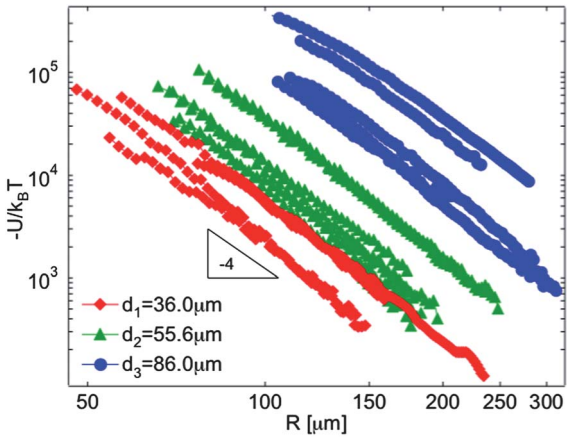

Fig. 11 Interaction potential (U/k_BT) between pairs of equally sized Janus bubbles as a function of inter-bubble distance (R). d_i is the diameter of Janus bubbles. Reprinted with permission from ref. 75.

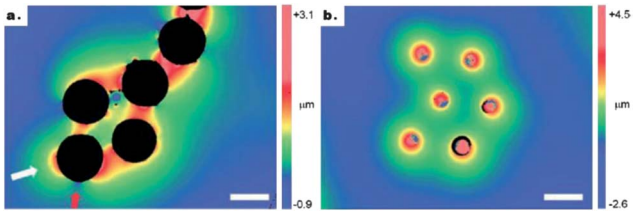

Fig. 12 Profilometry contour plots show difference in interfacial deformation around (a) Janus bubbles and (c) unmodified bubbles. White arrow indicates positive capillary charge (positive deformation) and red arrow indicates negative deformation (scale bar is 50 μm). Reprinted in part with permission from ref. 75.

properties will influence the stability of emulsions and foams stabilized by Janus particles. In addition, tuning and controlling the shape and magnitude of Janus boundary undulation possibly provides a new bottom-up method to generate a variety of two-dimensional "super-structures" made of Janus particles at the fluid interfaces.

Non-spherical Janus particles at fluid–fluid interfaces

So far, we have summarized the recent developments in understanding the behaviour of spherical Janus particles at fluid–fluid interfaces. Considering that a variety of techniques have been developed to prepare complex Janus particles with geometric anisotropy,[30,56,78–89] it is interesting to consider the possibility of investigating the effect of shape on the behaviour of Janus particles at fluid–fluid interfaces. More importantly, the control over chemical and geometrical anisotropy potentially provides a method to emulate the rich behaviour of molecular surfactants at fluid interfaces. For example, it is well known that the surface activity of molecular surfactants depends strongly on their molecular structure and chemical amphiphilicity, which are quantified in terms of the packing parameter and the hydrophile–lipophile balance (HLB) number, respectively. It can be imagined that the shape and chemistry of non-spherical Janus particles would play crucial roles in determining their properties as colloid surfactants in stabilizing various multiphasic mixtures such as emulsions and foams. For example, Janus dumbbells comprising two partially fused spheres offer new opportunities in independently controlling the chemistry and the size ratio of the two spheres (Fig. 4). In this section, we review recent work on the configuration behaviour of individual non-spherical Janus particles at fluid–fluid interfaces and on the assembly structures and interparticle interactions between non-spherical Janus particles at fluid interfaces. We note that significant efforts have been recently devoted to understanding the behaviour of chemically homogenous non-spherical particles at fluid interfaces and these reports have been summarized in a comprehensive review by Botto *et al.*[87]

Our group recently studied the configuration (*i.e.*, orientation and vertical displacement) of two types of non-spherical Janus particles at fluid–fluid interfaces: ellipsoids and dumbbells shown in Fig. 13. The attachment energy calculation and the subsequent energy minimization as a function of the orientation angle (θ_r) and the vertical displacement (d_v) facilitate the determination of the equilibrium configuration of individual Janus particles.[90,91] These calculations were performed with the assumption of a flat interface, which was shown to be a reasonable approximation that facilitates the determination of the orientation phase diagram.[91] The attachment energy of a non-spherical Janus particle from water or oil to a planar oil–water interface is given by,[4,61,90–92]

$$\Delta E_{Iw} = \gamma_{ow}(S_{Ao}\cos\theta_A + S_{Po}\cos\theta_P - S_I) \text{ from the water phase} \quad (8)$$

$$\Delta E_{Io} = -\gamma_{ow}(S_{Aw}\cos\theta_A + S_{Pw}\cos\theta_P + S_I) \text{ from the oil phase} \quad (9)$$

where γ_{ow} is the interfacial tension, S_{ij} is the surface area of each region of the particle (i = A or P) in contact with each fluid phase (j = w or o), and θ is the three-phase contact angle. The subscripts, A and P, indicate the apolar and polar surfaces of the particle, and o and w denote oil and water, respectively. S_I is the area of the interface displaced by the presence of the particle. The calculation of each surface area (S_{ij}) was computed

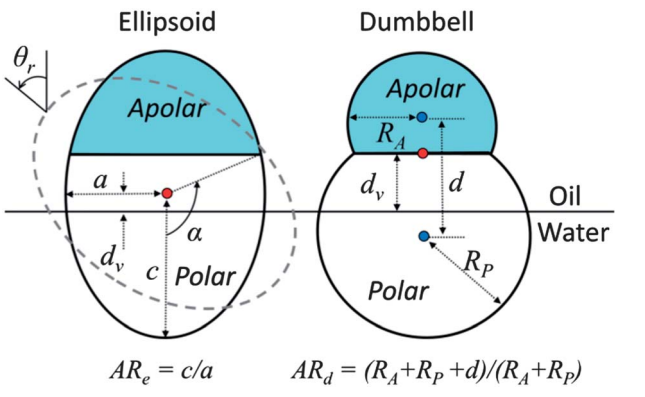

Fig. 13 Geometry of a Janus ellipsoid and a Janus dumbbell. Modified and reprinted from ref. 90.

by using a numerical method.[90,91] In this calculation, it was assumed that the contact line between the particle and the interface is smooth. The effect of line tension at the three-phase contact line is negligible for particles that are larger than a few nanometer in size. Gravity-induced interface deformation is also negligible in the small Bond number regime.

The geometric and chemical anisotropy of non-spherical Janus particles (*i.e.*, Janus ellipsoids and Janus dumbbells) was found to significantly influence their equilibrium configurations at the fluid–fluid interface.[90,91] The chemical anisotropy of a Janus particle favours the so-called upright configuration. For instance, a spherical Janus particle (chemically anisotropic spheres) trapped at the interface adopts the upright configuration, in which each hemisphere is exposed to its preferred fluid phase and the wettability separation line (WSL) between the two hemispheres coincides with the interface.[4,61,65] In this case, the Janus sphere tends to minimize the attachment energy by maximizing the values of S_{Ao} and S_{Pw}. In contrast, chemically isotropic but geometrically anisotropic particles prefer to adopt a configuration that maximizes the displaced area at the fluid interface due to the presence of the particles (S_I). For example, chemically homogenous ellipsoids and cylinders exhibit horizontal configurations at fluid–fluid interfaces.[93–95] Non-spherical Janus particles, thus, possess these two factors simultaneously, which compete with each other to determine their configuration at the fluid interface.

To quantitatively understand the effect of geometrical and chemical parameters on the configuration behaviours, the attachment energy was numerically calculated as a function of the orientation angle for symmetric Janus ellipsoids ($\alpha = 90°$) with a supplementary wetting condition (*i.e.*, $\beta = \theta_A - 90° = 90° - \theta_P$).[91] As shown in Fig. 14, for Janus ellipsoids with low aspect ratios at a constant wettability of $\beta = 30°$ (Fig. 14(a)), or with a strong wettability difference (*i.e.*, β) for a given aspect ratio, $AR_e = 5$ (Fig. 14(b)), the ellipsoids adopt the upright configuration (*i.e.*, $\theta_r = 0$). In contrast, Janus ellipsoids with high aspect ratios and/or a small wettability difference, the particles adopt tilted orientations at equilibrium. Interestingly, secondary energy minima in the attachment energy profiles were found under certain circumstances, such as high AR_e (Fig. 14(a)) or low β (Fig. 14(b)). The presence of a secondary energy minimum implies that the particles can be kinetically trapped in a metastable configuration. Based on this approach, the orientation phase diagrams for Janus ellipsoids and Janus dumbbells were obtained by varying the values of AR_e and β.

In general, as shown in the orientation phase diagrams in Fig. 15, Janus ellipsoids and Janus dumbbells adopt the upright configuration at the oil–water interface when the wettability difference (β) between the two regions is large or when the particle aspect ratio is close to AR = 1 (*i.e.*, Janus sphere).[91] In contrast, in the case of Janus particles with a weak wettability difference or a large aspect ratio, they exhibit tilted orientations with respect to the interface. As mentioned previously, under certain circumstances for Janus ellipsoids, the particles can be kinetically trapped in a metastable configuration due to the presence of a secondary energy minimum in the attachment energy profile, suggesting the co-existence of upright and tilted configurations (Fig. 15(a)).[91] Janus dumbbells, however, are not expected to adopt a metastable configuration because of the "thin waist" at the boundary between the two fused spheres (Fig. 15(b)).[91] Interestingly, when the size or wettability of the two spheres is significantly different, intermediate configurations are present in which the particle can freely rotate within a range of orientation angles.[90]

More recently, the configuration and assembly of non-spherical Janus particles were experimentally and numerically studied by spreading Janus cylinders at an oil–water interface.[97] These Janus cylinders were synthesized by using a micromolding method.[89] It was observed that Janus cylinders with a small aspect ratio adopt the upright configuration at the decane–water interface in which the WSL is pinned at the interface (Fig. 16(a) and (b)). For large aspect ratio particles, Janus cylinders possess either the upright or tilted configurations (Fig. 16(c) and (d)). Similar to the case of Janus ellipsoids, such co-existing configurations indicate the presence of two minima in the attachment energy profile (Fig. 16(e) and (f)), which was confirmed *via* numerical calculations. Excellent agreement between the experimental and numerical results again validated the flat interface assumption that was used to theoretically determine the equilibrium and metastable configurations of these Janus cylinders.

Such unique configuration behaviours of Janus cylinders significantly affect the assembly structure and the inter-particle interactions.[97] It was found that the pinned-upright

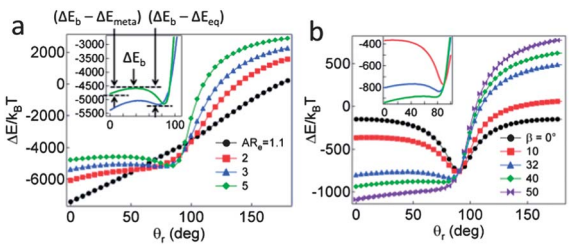

Fig. 14 Effect of the aspect ratio (AR_e) and the wettability (β) on the configuration behaviour of symmetric Janus ellipsoids with $c = 10$ nm at the decane–water interface: (a) $\beta = 30°$ and (b) $AR_e = 5$. The inset indicates a magnified plot to illustrate the magnitude of the energy barrier between equilibrium and metastable configurations. Modified and reprinted with permission from ref. 91.

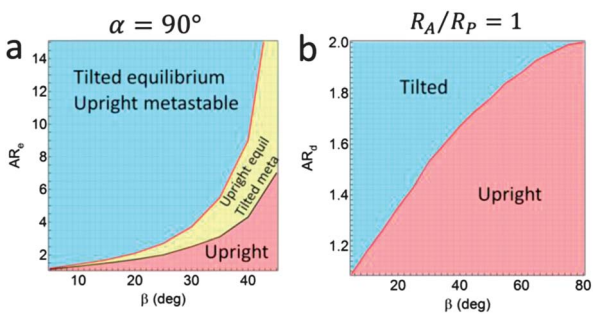

Fig. 15 Orientation phase diagrams for (a) Janus ellipsoids and (b) Janus dumbbells. Modified and reprinted with permission from ref. 91.

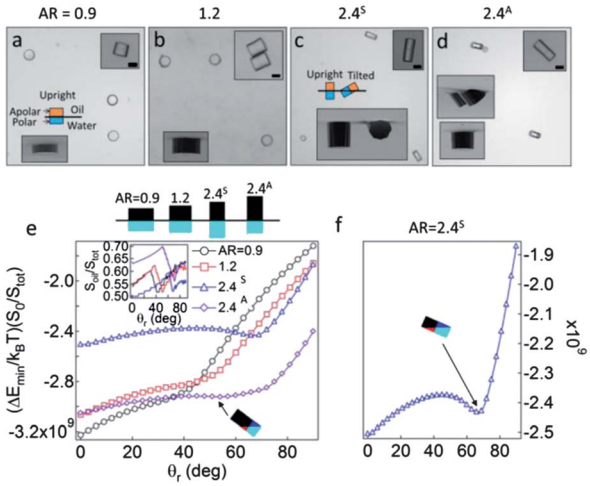

Fig. 16 (a–d) Effect of the aspect ratio (AR) on configurations of Janus cylinders at the decane–water interface. The superscripts, A and S, indicate that the ratios of polar and apolar regions are asymmetric and symmetric, respectively. The insets on the top right are the optical microscope images of the particles in water. The scale bar is 25 μm. The insets on the bottom left are the SEM images of PDMS replica prepared by the gel trapping method[96] in which the particle is partially embedded in the PDMS slab. (e) Attachment energy profiles as a function of the orientation angle (θ_r). (f) Attachment energy profile to show a secondary energy minimum. Modified and reprinted from ref. 97.

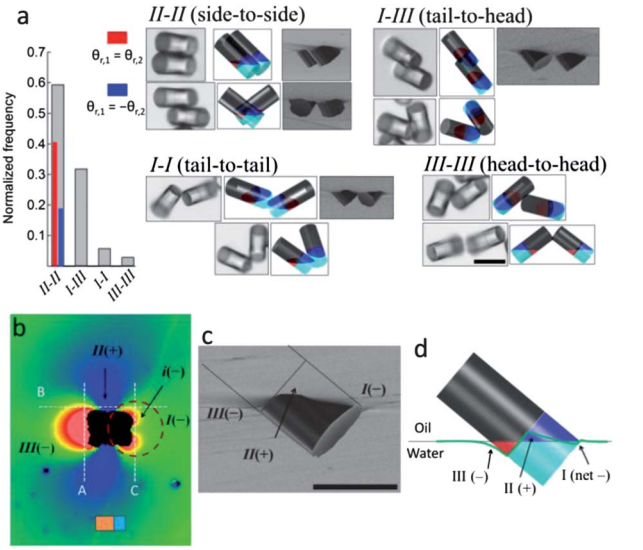

Fig. 17 (a) Histogram of lateral assemblies between two tilted Janus cylinders with AR = 2.4^A, and the corresponding snapshots, schematics and SEM images, if available. The scale bar is 50 μm. (b) Profilometry image of a tilted particle showing the quasi–quadrupolar interface deformation. (c) The corresponding SEM image on a PDMS slab. The scale bar is 30 μm. (d) Schematic of the titled particle with a deduced interface deformation. Modified and reprinted from ref. 97.

configuration leads to a relatively flat interface around Janus cylinders, resulting in negligible capillary interactions between them. In contrast, the interface around a tilted Janus cylinder is deformed in the shape of "quasi-quadrupole", as shown in Fig. 17(b)–(d). A variety of possible combinations of alignments between the quasi-quadrupoles of two tilted Janus cylinders result in the formation of diverse pair assembly structures as seen in Fig. 17(a). This diversity significantly differs from the assembly structures of homogenous cylinders and ellipsoids (*e.g.*, side-to-side and/or tip-to-tip), which tend to be highly deterministic.[87,93–95,98–100]

The complex interface deformation around Janus cylinders influences the inter-particle potential, which was found to depend on the lateral alignment between two cylinders.[97] As shown in Fig. 18(a) and (b), when two particles approach in the side-to-side alignment, the separation (r) between the particles as a function of time scales as $(t_{max} - t)^{\alpha}$ where t_{max} is the time when the particles make contact. The fitted value of α is about 0.167, which is related to the power law exponent, $\beta = 2 - 1/\alpha \approx -4$, for the pair interaction force, $F \sim r^{\beta-1}$,[94,97] which is similar to the capillary interactions between two homogenous spherical particles caused by quadrupolar interface deformation.[72,74] When a pair of particles approach each other in other alignments, however, the obtained value of α varies from 0.128 ($\beta \approx -5.8$) to 0.156 ($\beta \approx -4.4$), as seen in Fig. 18(c) and (d), suggesting a possible contribution of the hexapolar character of the interface deformation in Fig. 17b.

The assembly behaviours of non-spherical Janus particles at a fluid–fluid interface and the resulting interface-stabilization have recently been reported, based on dynamic surface tension measurements and computer simulations.[83] It was found that the adsorption kinetics and packing behaviours of Janus particles (*i.e.*, spheres, discs, and cylinders) at a toluene–water interface strongly depend on their geometry (Fig. 19). For Janus spheres, Brownian diffusion to the interface is responsible for the rapid decrease in the surface tension in the early stage (Fig. 19) during which the adsorption of the particles

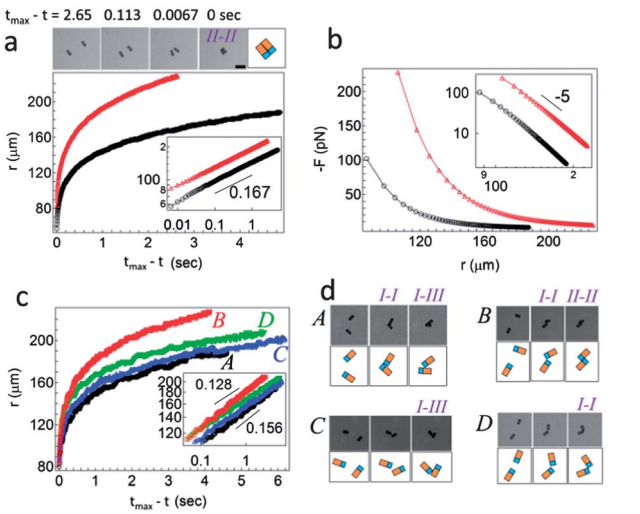

Fig. 18 Interactions between two tilted Janus cylinders with AR = 2.4^A at the decane–water interface. (a) Center-to-center separation, r, *versus* $(t_{max} - t)$ when the two particles approach side-to-side. Example snapshots are shown at the top. The scale bar is 50 μm. The schematic shows two assembled particles where the orange and light blue colors are apolar and polar regions, respectively. (b) Corresponding interaction force for the side-to-side approach. (c) Plot of r *versus* $(t_{max} - t)$ for four different pairs when two Janus cylinders approach in arbitrary alignments rather than in the side-to-side alignment. Insets in panel (a–c) are logarithmic plots. (d) Corresponding snapshots and schematics in the case of arbitrary approach. Reprinted from ref. 97.

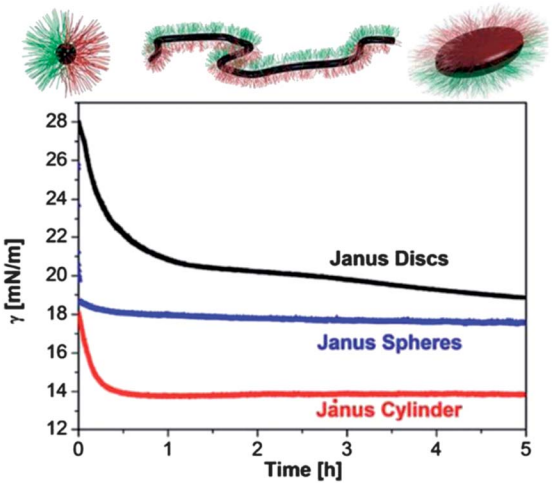

Fig. 19 Time evolution of the dynamic surface tension at the toluene–water interface upon the adsorption of non-spherical Janus particles. Modified and reprinted with permission from ref. 83.

spontaneously occurs (*i.e.*, diffusion controlled). As the surface coverage of the particles grows with time, the reduction in surface tension slows down because the pre-existing particles at the interface tend to prevent the additional adsorption of particles in the continuous phase (*i.e.*, collision controlled). For Janus discs, the evolution of the surface tension upon their adsorption to the interface differs from the case of Janus spheres. In the initial stage of the adsorption, the particles attach to the interface with either upright (primary energy minimum) or inverted (secondary energy minimum) orientation. Subsequently, the re-orientation or desorption process of the inverted particles accounts for the slower evolution in the surface tension, compared to that of Janus spheres (Fig. 19). In the case of flexible, chain-like Janus cylinders, these particles initially adsorb to the interface and form local domains. Subsequent in-plane and out-of-plane rearrangements upon the additional attachment lead to the formation of a liquid crystalline structure, which is not observed in the case of Janus spheres.

Conclusions and outlook

Janus particles combine the amphiphilicity of molecular surfactants and the strong interfacial attachment of colloidal particles, making them ideal candidates as solid surfactants for the stabilization of multiphasic mixtures such as emulsions and foams. As highlighted in this review, these amphiphilic Janus particles exhibit unique interfacial properties and behaviours that are not observed in homogenous particles. We hypothesize that the configuration of individual Janus particles influences the lateral interactions between multiple Janus particles and, in turn, affects the structure and properties of monolayers formed by multiple Janus particles at fluid interfaces. Ultimately, these interfacial behaviours will have a significant impact on their efficacy as solid surfactants. The recent surge in the detailed investigation of Janus particles at fluid interfaces is expected to lead to new insights that enable their widespread utilization in a variety of applications as emulsifiers and stabilizers in consumer products as well as advanced material processing.

A number of new possibilities in providing deeper understanding on the interfacial behaviour of Janus particles as well as enhancing the efficacy of Janus particles as solid surfactants exist. At the single particle level, it is still unclear what types of interactions govern the attachment of a Janus particle to a fluid–fluid interface. The dynamics of such a process warrants further study.[101] As discussed in this review, geometric anisotropy of Janus particles, in addition to their chemical anisotropy, provides an additional degree of freedom that allows for the control over the surface activity of Janus particles. Like molecular surfactants, the geometry of these non-spherical Janus particles could play a significant role in determining their efficacy as colloid surfactants for emulsion stabilization. Efforts to better define the geometric characteristics of these non-spherical Janus particles, analogous to the packing parameter of molecular surfactants, will enhance our ability to predict the behaviour of non-spherical particles for specific applications. Another important factor that may affect the effectiveness of non-spherical Janus particles as emulsifiers is the effect of interface curvature on their behaviour, which deserves a more in-depth investigation in the future. Also theoretical approaches to better understand the combined effect of chemical and geometrical anisotropy on the shape of interface deformation around non-spherical Janus particles warrant future investigation, because such interfacial deformation will have direct influence on the structure and properties of monolayers of these particles at the fluid interfaces. Simulations using software packages like Surface Evolver can further enhance our understanding of the assembly behaviour of multiple non-spherical Janus particles at fluid–fluid interfaces.[102] At the same time, it is essential to explore and exploit a wide variety of functional materials during synthesis of Janus particles, as it provides an added degree of freedom in modifying the properties and functionality of Janus particles for desired applications.

Another type of amphiphilic Janus particles that offers new possibilities are the so-called patchy particles, which have non-hemispherical patches that have different surface wettability than the rest of the particle surface.[11,76,103,104] Controlling the undulation of the wettability separation line (*i.e.*, Janus boundary) also will significantly affect the lateral interactions between these amphiphilic patchy particles at fluid interfaces. Techniques such as glancing angle deposition[103] and template-assisted fabrication[105] have been shown to produce amphiphilic patchy particles with controlled undulation in the wettability separation line (WSL). The WSL geometry likely will significantly influence the behavior of these particles at the interfaces. It is important to note that since studies involving fluid interfaces often involve large surface area (*e.g.*, emulsions), a large number of uniform particles will be required to enable systematic studies. Therefore, it will be extremely important to develop methods to produce uniform patchy particles with controlled undulations in large quantities.

The community would greatly benefit from studies focusing on the collective behaviours of Janus particles at fluid

interfaces. Namely, the rheological properties of Janus particle monolayers, which likely depend on the lateral interactions between Janus particles and the microstructure of the Janus particle monolayers, are expected to have a significant impact on the efficacy of Janus particles as emulsion stabilizers. Techniques such as interfacial rheometry,[106,107] and oscillating pendant drop tensiometry,[108] which have been successfully used to probe the properties of homogenous particle monolayers, provide unique opportunities to probe these important properties. Also a recently developed method to monitor the coalescence of particle-covered emulsion droplets at the droplet level will be extremely useful in testing the efficacy of Janus particles as emulsifiers.[109]

Another important outstanding question is revealing both the differences and the similarities between molecular surfactants and Janus particles as stabilizers for multiphasic mixtures.[61] Considering that many colloidal systems have been used as models for understanding atomic/molecular scale phenomena, it will be illuminating to test whether Janus particles serve as directly "observable" model systems for molecular surfactants.[110–112] While significant advances have been made in understanding the interfacial behaviour of Janus particles based on experimental and theoretical approaches, more computational methods to simulate the dynamic behaviour of Janus particles at interfaces would significantly benefit those in the field.

Acknowledgements

The authors acknowledge funding from the American Chemical Society Petroleum Research Fund (ACS PRF), NSF CAREER Award (DMR-1055594) and the PENN MRSEC DMR11-20901 through the NSF.

Notes and references

1 P. G. de Gennes, *Rev. Mod. Phys.*, 1992, **64**, 645–648.
2 C. Casagrande and M. Veyssié, *Acad. Sci., Paris, C. R.*, 1988, **306**, 1423–1425.
3 C. Casagrande, P. Fabre, E. Raphael and M. Veyssié, *Europhys. Lett.*, 1989, **9**, 251–255.
4 T. Ondarçuhu, P. Fabre, E. Raphaël and M. Veyssié, *J. Phys.*, 1990, **51**, 1527–1536.
5 J. di Meglio and E. Raphael, *J. Colloid Interface Sci.*, 1990, **136**, 581–583.
6 G. Rossmy, *Structure, Dynamics and Properties of Disperse Colloidal Systems*, 1998, vol. 111, pp. 17–26.
7 V. N. Paunov and O. J. Cayre, *Adv. Mater.*, 2004, **16**, 788–791.
8 A. Walther and A. H. E. Muller, *Soft Matter*, 2008, **4**, 663–668.
9 A. Perro, S. Reculusa, S. Ravaine, E. Bourgeat-Lami and E. Duguet, *J. Mater. Chem.*, 2005, **15**, 3745–3760.
10 S. Jiang, Q. Chen, M. Tripathy, E. Luijten, K. S. Schweizer and S. Granick, *Adv. Mater.*, 2010, **22**, 1060–1071.
11 A. B. Pawar and I. Kretzschmar, *Macromol. Rapid Commun.*, 2010, **31**, 150–168.
12 G. Loget and A. Kuhn, *J. Mater. Chem.*, 2012, **22**, 15457–15474.
13 C. Tang, C. Zhang, J. Liu, X. Qu, J. Li and Z. Yang, *Macromolecules*, 2010, **43**, 5114–5120.
14 S. Jiang, M. J. Schultz, Q. Chen, J. S. Moore and S. Granick, *Langmuir*, 2008, **24**, 10073–10077.
15 Z. Nie, W. Li, M. Seo, S. Xu and E. Kumacheva, *J. Am. Chem. Soc.*, 2006, **128**, 9408–9412.
16 S. C. Glotzer and M. J. Solomon, *Nat. Mater.*, 2007, **6**, 557–562.
17 R. Erhardt, M. Zhang, A. Boker, H. Zettl, C. Abetz, P. Frederik, G. Krausch, V. Abetz and A. H. E. Muller, *J. Am. Chem. Soc.*, 2003, **125**, 3260–3267.
18 R. Erhardt, A. Boker, H. Zettl, H. Kaya, W. Pyckhout-Hintzen, G. Krausch, V. Abetz and A. H. E. Muller, *Macromolecules*, 2001, **34**, 1069–1075.
19 D. Dendukuri, T. A. Hatton and P. S. Doyle, *Langmuir*, 2007, **23**, 4669–4674.
20 L. Hong, A. Cacciuto, E. Luijten and S. Granick, *Nano Lett.*, 2008, **6**, 2510–2514.
21 Q. Chen, J. K. Whitmer, S. Jiang, S. C. Bae, E. Luijten and S. Granick, *Science*, 2011, **331**, 199–202.
22 D. J. Kraft, R. Ni, F. Smallenburg, M. Hermes, K. Yoon, D. A. Weitz, A. van Blaaderen, J. Groenewold, M. Dijkstra and W. K. Kegel, *Proc. Natl. Acad. Sci. U. S. A.*, 2012, **109**, 10787–10792.
23 W. Gao, M. D'Agostino, G. Garcia, J. Orozco and J. Wang, *Small*, 2012, **9**, 467–471.
24 D. Patra, S. Sengupta, W. Duan, H. Zhang, R. Pavlick and A. Sen, *Nanoscale*, 2013, **5**, 1273–1283.
25 H.-R. Jiang, N. Yoshinaga and M. Sano, *Phys. Rev. Lett.*, 2010, **105**, 268302–268304.
26 L. F. Valadares, Y. G. Tao, N. S. Zacharia, V. Kitaev, F. Galembeck, R. Kapral and G. A. Ozin, *Small*, 2010, **6**, 565–572.
27 H. Ke, S. Ye, R. L. Carroll and K. Showalter, *J. Phys. Chem. A*, 2010, **114**, 5462–5467.
28 W. F. Paxton, S. Sundararajan, T. E. Mallouk and A. Sen, *Angew. Chem., Int. Ed.*, 2006, **45**, 5420–5429.
29 W. F. Paxton, K. C. Kistler, C. C. Olmeda, A. Sen, S. K. S. Angelo, Y. Cao, T. E. Mallouk, P. E. Lammert and V. H. Crespi, *J. Am. Chem. Soc.*, 2004, **126**, 13424–13431.
30 K.-H. Roh, D. C. Martin and J. Lahann, *Nat. Mater.*, 2005, **4**, 759–763.
31 J. R. Howse, R. A. L. Jones, A. J. Ryan, T. Gough, R. Vafabakhsh and R. Golestanian, *Phys. Rev. Lett.*, 2007, **99**, 048102–048104.
32 S. J. Ebbens and J. R. Howse, *Soft Matter*, 2010, **6**, 726–738.
33 Y. Zhang, H. F. Chan and K. W. Leong, *Adv. Drug Delivery Rev.*, 2012, **65**, 104–120.
34 W. Li, Y. Liu, G. Brett and J. D. Gunton, *Soft Matter*, 2012, **8**, 6027–6032.
35 D. A. Hays, *J. Electrost.*, 2001, **51**, 57–63.
36 D. Suzuki and H. Kawaguchi, *Colloid Polym. Sci.*, 2006, **284**, 1471–1476.
37 T. Nisisako, T. Torii, T. Takahashi and Y. Takizawa, *Adv. Mater.*, 2006, **18**, 1152–1156.
38 S. Gangwal, O. J. Cayre and O. D. Velev, *Langmuir*, 2008, **24**, 13312–13320.

39 J. M. Crowley, N. K. Sheridon and L. Romano, *J. Electrost.*, 2002, **55**, 247–259.
40 B. H. McNaughton, R. R. Agayan, J. X. Wang and R. Kopelman, *Sens. Actuators, B*, 2007, **121**, 330–340.
41 M. D. McConnell, M. J. Kraeutler, S. Yang and R. J. Composto, *Nano Lett.*, 2010, **10**, 603–609.
42 S. H. Kim, S. J. Jeon, W. C. Jeong, H. S. Park and S. M. Yang, *Adv. Mater.*, 2008, **20**, 4129–4134.
43 C. J. Behrend, J. N. Anker, B. H. McNaughton, M. Brasuel, M. A. Philbert and R. Kopelman, *J. Phys. Chem. B*, 2004, **108**, 10408–10414.
44 C. J. Behrend, J. N. Anker, B. H. McNaughton and R. Kopelman, *J. Magn. Magn. Mater.*, 2005, **293**, 663–670.
45 M. A. Bucaro, P. R. Kolodner, J. A. Taylor, A. Sidorenko, J. Aizenberg and T. N. Krupenkin, *Langmuir*, 2008, **25**, 3876–3879.
46 A. Synytska, R. Khanum, L. Ionov, C. Cherif and C. Bellmann, *ACS Appl. Mater. Interfaces*, 2011, **3**, 1216–1220.
47 S. H. Kim, S. Y. Lee and S. M. Yang, *Angew. Chem., Int. Ed.*, 2010, **49**, 2535–2538.
48 B. P. Binks, *Curr. Opin. Colloid Interface Sci.*, 2002, **7**, 21–41.
49 J. Faria, M. P. Ruiz and D. E. Resasco, *Adv. Synth. Catal.*, 2010, **352**, 2359–2364.
50 J. Hu, S. Zhou, Y. Sun, X. Fang and L. Wu, *Chem. Soc. Rev.*, 2012, **41**, 4356–4378.
51 C. Kaewsaneha, P. Tangboriboonrat, D. Polpanich, M. M. Eissa and A. Elaissari, *ACS Appl. Mater. Interfaces*, 2013, **5**, 1857–1869.
52 M. Oettel and S. Dietrich, *Langmuir*, 2008, **24**, 1425.
53 B. P. Binks and T. S. Horozov, *Colloidal Particles at Liquid Interfaces*, Cambridge University Press, 2006.
54 N. Glaser, D. J. Adams, A. Boker and G. Krausch, *Langmuir*, 2006, **22**, 5227–5229.
55 Y. K. Takahara, S. Ikeda, S. Ishino, K. Tachi, K. Ikeue, T. Sakata, T. Hasegawa, H. Mori, M. Matsumura and B. Ohtani, *J. Am. Chem. Soc.*, 2005, **127**, 6271–6275.
56 J.-W. Kim, D. Lee, H. C. Shum and D. A. Weitz, *Adv. Mater.*, 2008, **20**, 3239–3243.
57 A. F. Mejia, A. Diaz, S. Pullela, Y. W. Chang, M. Simonetty, C. Carpenter, J. D. Batteas, M. S. Mannan, A. Clearfield and Z. Cheng, *Soft Matter*, 2012, **8**, 10245–10253.
58 A. Walther, K. Matussek and A. H. E. Müller, *ACS Nano*, 2008, **2**, 1167–1178.
59 A. Walther, M. Hoffmann and A. H. E. Müller, *Angew. Chem., Int. Ed.*, 2007, **120**, 723–726.
60 H. Fan and A. Striolo, *Soft Matter*, 2012, **8**, 9533–9538.
61 B. P. Binks and P. D. I. Fletcher, *Langmuir*, 2001, **17**, 4708–4710.
62 R. Aveyard, *Soft Matter*, 2012, **8**, 5233–5240.
63 J. N. Israelachvili, *Intermolecular and Surface Forces: Revised Third Edition*, Academic press, 2011.
64 D. J. Adams, S. Adams, J. Melrose and A. C. Weaver, *Colloids Surf., A*, 2008, **317**, 360–365.
65 S. Jiang and S. Granick, *J. Chem. Phys.*, 2007, **127**, 161102–161104.
66 D. L. Cheung and S. A. F. Bon, *Soft Matter*, 2009, **5**, 3969–3976.
67 Y. Hirose, S. Komura and Y. Nonomura, *J. Chem. Phys.*, 2007, **127**, 054707–054705.
68 J. Lucassen, *Colloids Surf.*, 1992, **65**, 139–149.
69 J. Lucassen, *Colloids Surf.*, 1992, **65**, 131–137.
70 B. J. Park, T. Brugarolas and D. Lee, *Soft Matter*, 2011, **7**, 6413–6417.
71 P. A. Kralchevsky and K. Nagayama, *Langmuir*, 1994, **10**, 23–36.
72 D. Stamou, C. Duschl and D. Johannsmann, *Phys. Rev. E: Stat. Phys., Plasmas, Fluids, Relat.*, 2000, **62**, 5263–5272.
73 P. A. Kralchevsky, N. D. Denkov and K. D. Danov, *Langmuir*, 2001, **17**, 7694–7705.
74 K. D. Danov, P. A. Kralchevsky, B. N. Naydenov and G. Brenn, *J. Colloid Interface Sci.*, 2005, **287**, 121–134.
75 T. Brugarolas, B. J. Park and D. Lee, *Adv. Funct. Mater.*, 2011, **21**, 3924–3931.
76 A. B. Pawar and I. Kretzschmar, *Langmuir*, 2009, **25**, 9057–9063.
77 M. Conradi, M. Ravnik, M. Bele, M. Zorko, S. Zumer and I. Musevic, *Soft Matter*, 2009, **5**, 3905–3912.
78 O. Güell, F. Sagués and P. Tierno, *Adv. Mater.*, 2011, **23**, 3674–3679.
79 Y. Hong, N. M. K. Blackman, N. D. Kopp, A. Sen and D. Velegol, *Phys. Rev. Lett.*, 2007, **99**, 178103–178104.
80 J.-W. Kim, R. J. Larsen and D. A. Weitz, *J. Am. Chem. Soc.*, 2006, **128**, 14374–14377.
81 D. Lee and D. A. Weitz, *Small*, 2009, **5**, 1932–1935.
82 T. M. Ruhland, A. H. Gröschel, A. Walther and A. H. E. Müller, *Langmuir*, 2011, **27**, 9807–9814.
83 T. M. Ruhland, A. H. Gröschel, N. Ballard, T. S. Skelhon, A. Walther, A. H. E. Müller and S. A. F. Bon, *Langmuir*, 2013, **29**, 1388–1394.
84 B. Wang, B. Li, R. C. M. Ferrier and C. Y. Li, *Macromol. Rapid Commun.*, 2010, **31**, 169–175.
85 Z. Zhang, P. Pfleiderer, A. B. Schofield, C. Clasen and J. Vermant, *J. Am. Chem. Soc.*, 2010, **133**, 392–395.
86 E. B. Mock, H. De Bruyn, B. S. Hawkett, R. G. Gilbert and C. F. Zukoski, *Langmuir*, 2006, **22**, 4037–4043.
87 L. Botto, E. P. Lewandowski, M. Cavallaro and K. J. Stebe, *Soft Matter*, 2012, **8**, 9957–9971.
88 M. R. Buck, J. F. Bondi and R. E. Schaak, *Nat. Chem.*, 2012, **4**, 37–44.
89 C.-H. Choi, J. Lee, K. Yoon, A. Tripathi, H. A. Stone, D. A. Weitz and C.-S. Lee, *Angew. Chem., Int. Ed.*, 2010, **49**, 7748–7752.
90 B. J. Park and D. Lee, *Soft Matter*, 2012, **8**, 7690–7698.
91 B. J. Park and D. Lee, *ACS Nano*, 2012, **6**, 782–790.
92 S. Jiang and S. Granick, *Langmuir*, 2008, **24**, 2438–2445.
93 E. P. Lewandowski, P. C. Searson and K. J. Stebe, *J. Phys. Chem. B*, 2006, **110**, 4283–4290.
94 J. C. Loudet, A. M. Alsayed, J. Zhang and A. G. Yodh, *Phys. Rev. Lett.*, 2005, **94**, 018301–018304.
95 B. Madivala, J. Fransaer and J. Vermant, *Langmuir*, 2009, **25**, 2718–2728.
96 V. N. Paunov, *Langmuir*, 2003, **19**, 7970–7976.

97 B. J. Park, C.-H. Choi, S.-M. Kang, K. E. Tettey, C.-S. Lee and D. Lee, *Soft Matter*, 2013, **9**, 3383–3388.
98 L. Botto, L. Yao, R. L. Leheny and K. J. Stebe, *Soft Matter*, 2012, **8**, 4971–4979.
99 E. P. Lewandowski, M. Cavallaro, L. Botto, J. C. Bernate, V. Garbin and K. J. Stebe, *Langmuir*, 2010, **26**, 15142–15154.
100 J. C. Loudet and B. Pouligny, *Europhys. Lett.*, 2009, **85**, 28003.
101 D. M. Kaz, R. McGorty, M. Mani, M. P. Brenner and V. N. Manoharan, *Nat. Mater.*, 2011, **11**, 138–142.
102 H. Rezvantalab and S. Shojaei-Zadeh, *Soft Matter*, 2013, **9**, 3640–3650.
103 A. B. Pawar and I. Kretzschmar, *Langmuir*, 2008, **24**, 355–358.
104 E. Bianchi, R. Blaak and C. N. Likos, *Phys. Chem. Chem. Phys.*, 2011, **13**, 6397–6410.
105 Z. He and I. Kretzschmar, *Langmuir*, 2012, **28**, 9915–9919.
106 C. F. Brooks, G. G. Fuller, C. W. Frank and C. R. Robertson, *Langmuir*, 1999, **15**, 2450–2459.
107 S. Reynaert, C. F. Brooks, P. Moldenaers, J. Vermant and G. G. Fuller, *J. Rheol.*, 2008, **52**, 261–285.
108 D. O. Johnson and K. J. Stebe, *J. Colloid Interface Sci.*, 1994, **168**, 21–31.
109 A. B. Pawar, M. Caggioni, R. Ergun, R. W. Hartel and P. T. Spicer, *Soft Matter*, 2011, **7**, 7710–7716.
110 D. G. A. L. Aarts, M. Schmidt and H. N. W. Lekkerkerker, *Science*, 2004, **304**, 847–850.
111 W. Poon, *Science*, 2004, **304**, 830–831.
112 W. Poon, *J. Phys.: Condens. Matter*, 2002, **14**, R859.